Salvadora Persica branches biomass adsorbent for removal of uranium(VI) and thorium(IV) from aqueous solution: kinetics and thermodynamics study

Mazen K. Nazal[1] · Mohammad Al-Bayyari[2] · Fawwaz I. Khalili[3]

Abstract

Adsorption isotherms of U(VI) and Th(IV) in water were obtained and removal kinetics was studied. The main functional groups on the surface of *Salvadora Persica* branches adsorbent were identified using a Fourier-transform infrared and the surface morphology of adsorbent was characterized by a Scanning Electron Microscope. Effects of the U(VI) and Th(IV) initial concentrations, contact time, the mass of adsorbent loading, pH of the solution were investigated at 25 ± 0.3 °C. The efficiencies with which this adsorbent removes U(VI) and Th(IV) from their solutions in water are reported. The adsorption isotherm fitted the Freundlich model. The adsorption of U(VI) and Th(IV) follows the pseudo-second order kinetic with squared correlation coefficients (R^2) close to 1.0. The thermodynamic parameters (i.e. the free energy (ΔG^o_{ads}), the enthalpy (ΔH^o_{ads}) and the entropy of adsorption (ΔS^o_{ads}) for the adsorption of U(VI) and Th(IV) on the *Salvadora Persica* branches adsorbent were reported.

Keywords Environment · Radioactive elements · Adsorption isotherms · Removal efficiency · Thermodynamic of adsorption

Introduction

The radioactive actinides such as uranium and thorium can be found in rocks, soil and groundwater. In addition, the main essential elements in the nuclear energy program are uranium and thorium. Uranium and thorium ions which exist in the environment are hazardous to the environment and human health due to their toxicity and radioactivity. The contaminated water with the uranium and thorium radioactive elements can cause many dangerous diseases and many biological studies have reported that these elements are considered as a carcinogen for the pancreas, kidney, lung, liver, immune-system and neuro-system [1, 2]. Moreover, separation, removal and purification of uranium and thorium ions from their ores and nuclear waste have become major topics and have attracted the attention of researchers in recent years. Therefore, and due to the safety regulations and economic benefits, the separation and removal of these radioactive ions are necessary and important to minimize their discharge into the environment. There are various techniques used for the removal and separation of the U(VI) and Th(IV) radioactive ions, such as solvent extraction, precipitation and ion exchange [3–6] and adsorption [7, 8]. The adsorption technique for removal and separation of U(VI) and Th(IV) radioactive ions from their host media using adsorbents is promising because of the following reasons; it is simple, highly efficient, cost-effective and environment friendly. In the last few years, many researchers have worked on developing various adsorbents for removal of U(VI) and Th(IV) ions such as activated carbon, cement, silica, zeolite, coir pith, clay minerals, bayberry tannin onto bovine serum albumin Nano-spheres [9] and natural organic matter [10, 11] were tested for that purpose. However, highly available and low-cost adsorbents with high removal capacities are still needed.

✉ Mazen K. Nazal
  mazennazal@kfupm.edu.sa

[1] Center for Environment and Water, Research Institute, King Fahd University of Petroleum and Minerals, Dhahran 31261, Saudi Arabia

[2] College of Science and Health Professions King Saud Bin Abdulaziz University for Health Sciences, National Guard Health Affairs, Jeddah, Saudi Arabia

[3] Department of Chemistry, Faculty of Science, The University of Jordan, Amman 11942, Jordan

Salvadora Persica branches (Miswak) are widely used in the Middle East and Eastern African cultures, as a chewing stick. It is obtained from the roots, twigs or stems of *Salvadora Persica* L trees. It is considered a green material and it has many biological effects, including anti-bacterial and anti-fungal properties. The *Salvadora Persica* branches contain several functional groups for binding metal ions. They mainly consist of saponins, tannins, silica and resin [12], which are contributing in the removal of ions such as Th(IV) and U(VI) from aqueous solutions. Ileri and Erduran in 2014 studied the removal of heavy metals from aqueous solutions by *Salvadora Persica* L. Branches waste [13]. Their results indicate that the *Salvadora Persica* branches waste may be used as a good and effective adsorbent for common heavy metals contaminants from the aqueous solution.

In this study, the adsorption capability of *Salvadora Persica* Branches material was investigated for the removal of the U(VI) and Th(IV) ions from aqueous solutions. Then to understand the adsorption behavior of these ions on the *Salvadora Persica* branches, the following parameters were studied; (i) the effect of pH, (ii) contact time, (iii) adsorbent dosage and (iv) initial ion concentrations. Different adsorption isotherms namely; the Langmuir, Freundlich, Temkin and Dubinin–Radushkevich (D–R) models were tested for fitting the experimental results. The kinetic and thermodynamic parameters of adsorption were also calculated.

Experimental

Treatment and characterization of adsorbent

Branches of *Salvadora Persica* were purchased from a local market in Saudi Arabia. The branches were crushed then the resulted powder was cleaned and washed by removing soluble and colored compounds using hexane, ethanol and hot DI water for 1 hour until a colorless solution of Miswak powder was observed. Without any further modification, the cleaned Miswak powder was dried overnight in an oven at 105 ± 0.3 °C then stored in a clean glass vial to be used later in the adsorption experiments. FTIR (Nicolet 6700 Thermo Electron) instrument was used for the functional groups characterization, the thermal stability of the material under air and nitrogen was tested using the thermal gravimetric analysis (TGA Q500, TA Instruments, USA), and the adsorbent surface morphology and its elemental composition were characterized using the Scanning Electron Microscope (SEM) and Energy Dispersive X-ray Spectroscopy (EDX) respectively. The automated gas sorption analyzer (Autosorb iQ Quantachrome USA) was used to analyze the surface area and porosity of the adsorbent.

Preparation of solutions

Indicator solution

A 0.1% of Arsenazo (III) indicator solution was prepared by dissolving 0.1 g in deionized water (100 mL) for spectrophotometric determination of U(VI) and Th(IV) before and after the adsorption.

Thorium (IV) and Uranium (VI) Stock Solutions

A stock solution of U(VI) and Th(IV) ions were prepared separately by dissolving an exact amount of uranyl nitrate hexahydrate or thorium nitrate tetrahydrate salt in deionized water to get a concentration of 2000 µg/mL for each metal. Later these two stock solutions were used to prepare a different concentrations series (5.0–80 µg/mL) of U(VI) and Th(IV) in 1.0×10^{-4} M HCl. These diluted solutions were used to construct two separated standard calibration curves for U(VI) and Th(IV) concentration determination (shown in Fig. 1) using a UV-spectrophotometer (Spectroscan DU). The spectrophotometric method of determination of U(IV) and Th(IV) was described elsewhere [14]. Briefly, for U(VI) ions determination, a 0.5 mL of Arsenazo (III) indicator was added to 25 mL volumetric flask contains 2.0 mL of uranium solution and 10 mL of 0.01 M HCl then the volume was completed to the mark with deionized water. A few milliliters of solution were used in the spectrophotometric measurement which was carried out at 25 ± 0.3 °C and at 650 nm wavelength. For Th(IV) ions determination, 0.5 mL of Arsenazo (III) indicator was added to a 0.5 mL Th(IV) solution and 10 mL of 9 M HCl in a 25 mL volumetric flask then the volume was completed by deionized water. All the spectrophotometric measurements were carried out at 25 ± 0.3 °C and at 660 nm wavelength.
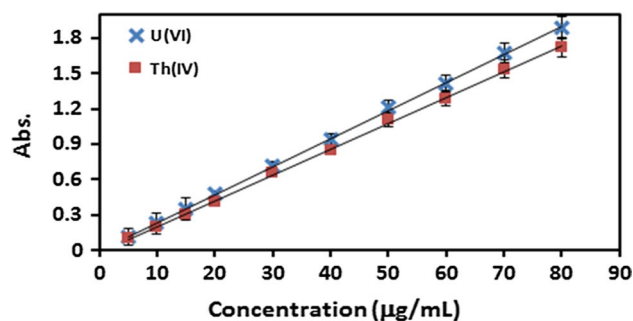

Fig. 1 U(VI) and Th(IV) standard calibration curves

Batch adsorption experiments

The effect of pH, adsorbent dosage, contact time and the concentration of U(VI) and Th(IV) ions on the uptake of U(VI) and Th(IV) ions by the *Salvadora Persica* branches adsorbent were studied in a batch mode at 25 ± 0.3 °C. To evaluate the effect of pH on the adsorption process, 60 μg/mL of metal ions concentration were prepared in solutions had different pH values (i.e. 0.5, 1, 2, 3 and 4). A 1.25 g of the adsorbent was added to 50 mL of the solution, then agitated at 150 rpm using water bath shaker (Memmert GmbH Instrument Germany) for 4 h then allowed to settle. The effect of adsorbent dosage on the removal of the U(VI) or Th(IV) solution has pH 4 and containing 60 μg/mL of each of them was studied at constant temperature of 25 °C by varying the added mass of adsorbent from 0.01 to 2.00 g and shaking the mixture for 4 h. The effect of U(VI) or Th(IV) concentration (i.e. 20, 30, 40, 50, 60, 70 and 80 μg/mL) in 50 mL solution on their removal by 1.25 g of adsorbent was investigated at 25 ± 0.3 °C. For studying the U(VI) and Th(IV) ions adsorption kinetic using 1.25 g adsorbent, a 50 mL of solutions has a pH 4 and containing 60 μg/mL of U(VI) or Th(IV) were studied by agitation these solutions at 150 rpm and 25 ± 0.3 °C for different time intervals of 15, 30, 45, 60, 120, 240, 480, 960 and 1440 min. The thermodynamic adsorption of 60 μg/mL U(VI) or Th(IV) on 1.25 g of adsorbent was studied by agitating these solutions for 4 hours at different temperatures (i.e. 25, 30, 35 and 40 ± 0.3 °C).

In all the adsorption experiments, the solutions were filtered and the concentration of U(VI) and Th(IV) at equilibrium (C_e) was measured using the previously described spectrophotometric method in Sect. 2.2.2. The adsorbed amount of U(VI) and Th(IV) by *Salvadora Persica* branches powder (q_e) in the mg/g unit was calculated using the following Eq. (1);

$$q_e = \frac{(C_0 - C_e)}{m} \times V \tag{1}$$

where C_0 is the initial concentration (μg/mL) of U(VI) or Th(IV) ions, C_e is the concentration (μg/mL) of U(VI) and Th(IV) at equilibrium, V is the volume (L) of the solution

and m is the mass (g) of adsorbent in g. The percentage of removal (%) was calculated using Eq. 2

$$\text{Removal } \% = \frac{C_0 - C_e}{C_0} \% \tag{2}$$

Adsorption isotherms

The equilibrium data of U(VI) and Th(IV) ions adsorption on the adsorbent was tested by various frequently used adsorption isotherms models (summarized in Table 1). Freundlich isotherm [15] is an empirical model has been established by assuming the surface of the adsorbent is heterogeneous and the adsorption sites have different affinities to the adsorbate molecules. It also describes the multilayer adsorption and assumes the adsorption process is reversible. The Langmuir isotherms [16] describe the relationship between the adsorbed analyte molecules and the concentration of that analyte at certain conditions. In the Langmuir model, a monolayer of adsorbate is formed on the surface of adsorbent, whereas it is assumed there is no any interaction or steric hindrance between the analyte molecules, as well as all the adsorption sites on the surface of adsorbent are identical with the same activation energy adsorption. Temkin is another model contains a factor describing the interaction between the adsorbate and adsorbent [17]. The forth adsorption isotherm model used in this study is Dubinin–Radushkevich isotherm [18]. This isotherm model is generally applied to express the adsorption mechanism with a Gaussian energy distribution onto a heterogeneous surface of adsorbent.

In these isotherm models (Freundlich, Langmuir, Temkin and Dubinin–Radushkevich (RD)), q_e is the adsorption capacity at equilibrium in mg/g, C_e is the concentration of U(VI) or Th(IV) in the solution at equilibrium in μg/mL, Q_0 is the maximum monolayer adsorption capacity in mg/g, and b is Langmuir constant in the Langmuir model. K_F and n are the Freundlich parameters where n is a measure of the heterogeneity of the surface of the adsorbent. In Temkin isotherm, b_T is the Temkin constant, R and T are the ideal gas constant in

Table 1 The original and linear forms of the most common four isotherm models mathematical equations

Isotherm	Non-Linear	Linear	Plot
Freundlich	$q_e = K_F C_e^{1/n}$	$\ln(q_e) = \ln(K_F) + \frac{1}{n}(C_e)$	$\ln(q_e)$ vs $\ln(C_e)$
Langmuir	$q_e = \frac{(Q_0 b C_e)}{1 + b C_e}$	$\frac{C_e}{q_e} = \frac{1}{bQ_0} + \frac{C_e}{Q_0}$	$\frac{C_e}{q_e}$ vs C_e
		$\frac{1}{q_e} + \frac{1}{Q_0} + \frac{1}{bQ_0 C_e}$	$\frac{1}{q_e}$ vs $\frac{1}{C_e}$
		$q_e = Q_0 - \frac{q_e}{bC_e}$	$\frac{1}{q_e}$ vs $\frac{q_e}{C_e}$
		$\frac{q_e}{C_e} = bQ_0 - bq_e$	$\frac{q_e}{C_e}$ vs q_e
Temkin	$q_e = \frac{RT}{b_T} \ln A_T C_e$	$q_e = \frac{RT}{b_T} \ln A_T + \frac{RT}{b_T} \ln C_e$	q_e vs $\ln C_e$
Dubinin–Radushkevich (R–D)	$q_e = Q_{\max} e^{-\beta \varepsilon^2}$	$\ln q_e = \ln Q_{\max} - \beta \varepsilon^2$	$\ln q_e$ vs $\ln \varepsilon^2$

J K^{-1} mol^{-1} and the temperature in Kelvin (K) respectively, and A_T is the isotherm binding constant in L/g. In D–R model, Q_{max} in mg/g is the maximum adsorption capacity of metal ions in the total specific micropores volume of the adsorbent, β is D–R isotherm constant (mol^2 kJ^{-2}) and ε is the D-R constant which is described by Eq. 3.

$$\varepsilon = RT \ln \left(1 + \frac{1}{C_e} \right) \tag{3}$$

This model gives an understanding about the mean free energy (E) of molecules adsorption (kJ/mol) and it is calculated by Eq. 4;

$$E = \frac{1}{\sqrt{2\beta_{DR}}} \tag{4}$$

Adsorption kinetics

To study the U(VI) and Th(IV) adsorption kinetics on *Salvadora Persica* branches adsorbent, a 50 mL of an aqueous solution with an initial concentration of 60 μg/mL of U(VI) or Th(IV) was added to 1.25 g of the adsorbent in a vial that was capped then shaken continuously for fixed time intervals (i.e. 15, 30, 45, 60 120, 240, 480, 960 and 1440 min). The adsorption results were fitted using the kinetic models reported by Lagergren and Ho [19, 20] that led to Eqs. (5) and (6) for, respectively, a pseudo-first order adsorption rate,

$$\ln (q_e - q_t) = \ln (q_e) - k_1 t \tag{5}$$

and a pseudo-second order adsorption rate,

$$\frac{t}{q_t} = \frac{1}{q_e^2 k_2} + \frac{t}{q_e} \tag{6}$$

where q_e is the adsorption capacity at equilibrium in mg/g, q_t in mg/g is the adsorption capacity at a time t (min), k_1 (min^{-1}) is the pseudo-first order rate constant and k_2 (g mg^{-1} min^{-1}) is the pseudo-second order rate constant.

Results and discussion

Characterization of *Salvadora Persica* branches adsorbent

The FTIR experiment was performed to characterize the surface's functional groups of the adsorbent. Figure 2 shows the IR spectrum for the adsorbent. The absorption between 3600 and 3000 cm^{-1} is due to the stretching, vibration and angular vibration of Hydroxyl (OH) and amine (NH$_2$) functional groups. The broad peak at around 3300 cm^{-1} was due the stretching vibration of the OH in the polysaccharide. The characteristic sharp peaks due to the stretching vibration of aliphatic C–H and the aromatic C=C are obvious at 2925 and 1618 cm^{-1} respectively. The peak between 2200 and 2400 cm^{-1} is due to the stretching vibration of C≡C and C≡N. The stretching of the C–O group gave a sharp peak at 1107 and 1022 cm^{-1}. This is all in line with the published literature [21].

Thermal analysis of adsorbent was performed using titanium pan with a sample weight of 10 mg under air and nitrogen at a flow rate of 30 mL/min and heating rate of 10 °C/min. Figure 3 shows three weight loss phases under air. The first phase took place at 207 °C with a loss of 9.4% of its mass, which was attributed to the volatile solvent and moisture removal. The second phase is due to the decomposing of *Salvadora Persica* branches material at 321 °C with a 54.6%
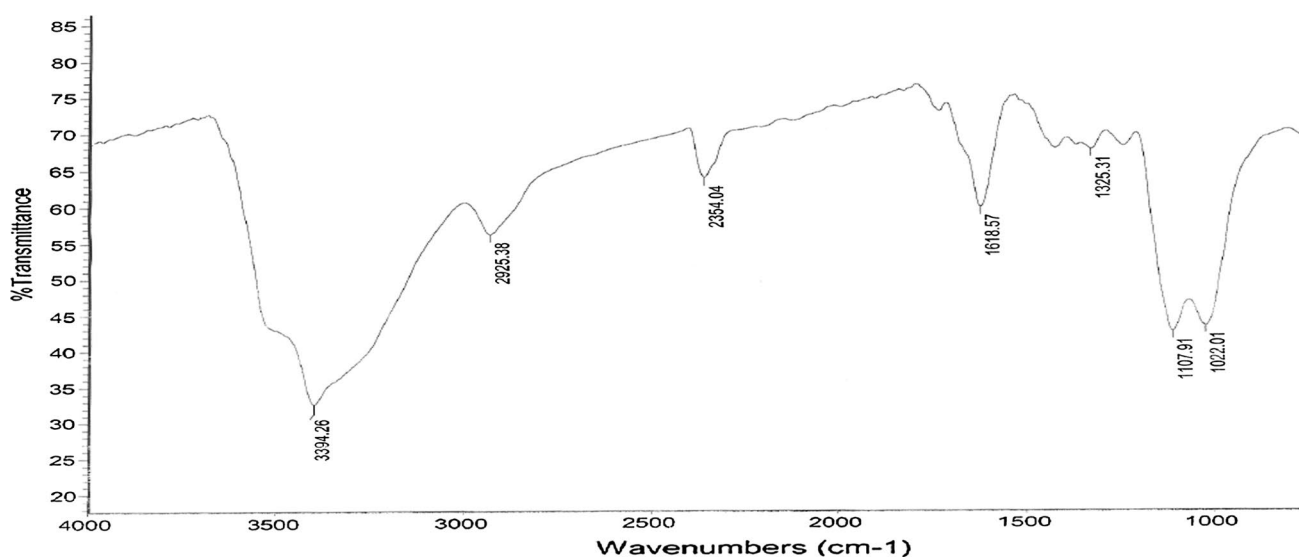

Fig. 2 FTIR spectrum of *Salvadora Persica* branches adsorbent

loss in mass and the third phase at 459 °C with 88.2% of loss is attributed to the oxidation of the adsorbent material. However, under nitrogen the thermal analysis shows two major mass loss phases at 319 °C and 900 °C with 51.24% and 84.5% weight loss, respectively, due to the decomposing and breaking down of the adsorbent material.

Figure 4a shows the surface morphology of the adsorbent powder. This material has rounded ends with a spongy structure. This structure in the adsorbent helps capturing the U(VI) and Th(IV) radioactive ions. These findings are in agreement with a study done by Nadia Halib et al. [22]. The EDX spectrum in the Fig. 4b shows the elemental composition of the adsorbent to be 58.5% carbon (C), 36.5% oxygen (O), 2.1% calcium (Ca), 1.5% potassium (K) and 1.4% sulfur (S).

The measured surface area and pore volume of the *Salvadora Persica* adsorbent are small (2.2 m^2/g) and the pore volume is 0.002 mL/g with a half pore width 16.57 Å. These finding can explain the relatively low adsorption capacity of the *Salvadora Persica* adsorbent for U(VI) and Th(IV) ions.

Effect of pH

The effect of pH is one of the significant factors that influence the adsorptive removal of metal ions from aqueous solutions. It influences the metals speciation as well as the active adsorption sites available on the surface of the adsorbents. The removal percentage values at 25 ± 0.3 °C were plotted against the corresponding initial pH values. Figure 5 shows that, as the pH increases from 0.5 to 3.0 the removal percentage of U(VI) and Th(IV) increases and reaches the maximum efficiency at pH 3.0. This can be attributed to the following two main reasons; (i) at pH less than 3, the concentration of H$^+$ ions is high and these ions compete with U(VI) and Th(IV) ions for the interacting with the active adsorption sites on the surface of *Salvadora Persica* adsorbent [23]. (ii) more extractable species of U(VI) and Th(IV) are formed at pH between 3 and 4 [24], whereas they show little tendency to be hydrolyzed. Therefore, a pH equal 4.0 ± 0.1 was chosen later in the adsorption experiments of U(VI) and Th(IV).

Fig. 3 Temperature versus wt.% loss of *Salvadora Persica* material under **a** air and **b** nitrogen
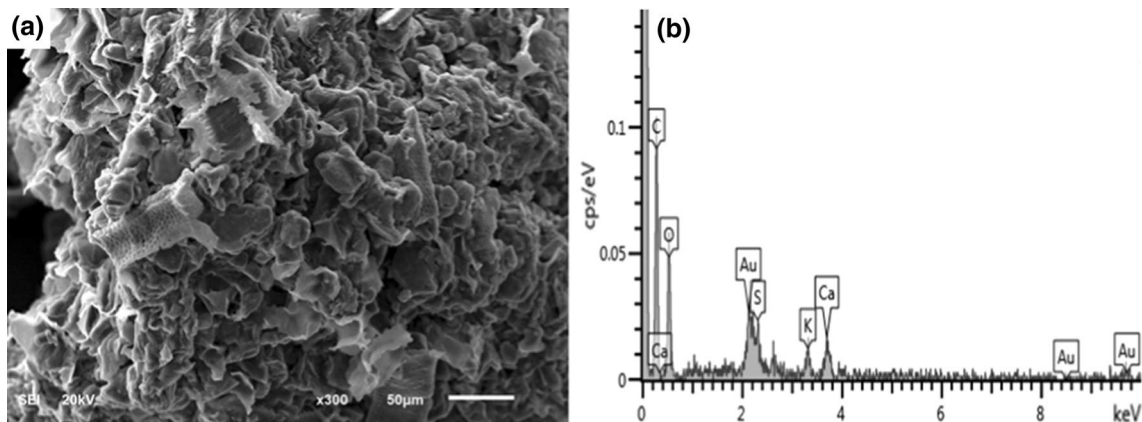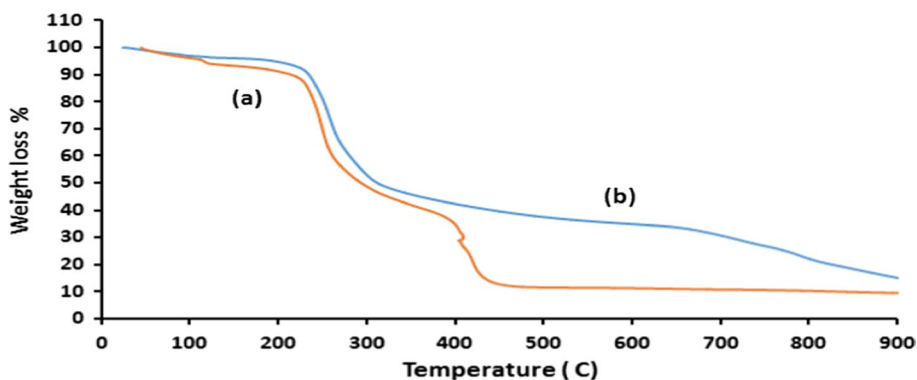

Fig. 4 **a** SEM image of *Salvadora Persica* adsorbent and **b** EDX spectrum
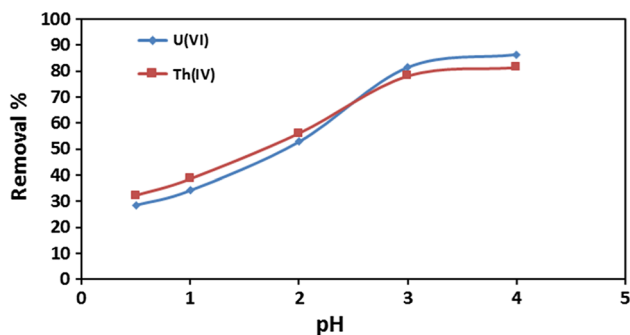
Fig. 5 Effect of pH on the removal percentage of U(VI) (60 μg/mL) and Th(IV) (60 μg/mL) using 1.25 g adsorbent at 25 ± 0.3 °C and contact time 4 h

Effect of adsorbent dosage

The effect of adsorbent mass on the removal of the U(VI) or Th(IV) solution at pH 4 and containing 60 μg/mL initial concentration was studied at constant temperature of 25 ± 0.3 °C by varying the added mass of *Salvadora Persica* adsorbent from 0.01 to 2.00 g and with contact time for 4 h. As shown in Fig. 6, the removal percentage of U(VI) and Th(IV) increased with the increase in the dosage of adsorbent. High removal percentage of U(VI) (around 85%) was found at adsorbent mass of 0.1 g, while the maximum removal of Th(IV) (80% removal) was found at the adsorbent dosage 0.5 g. The density of adsorption (q_e) showed opposite trend with adsorbent mass. This is attributed to the increase of adsorption sites with the increase of the adsorbent mass.

Table 2 shows a comparison between the adsorption capacity of the *Salvadora Persica* branches adsorbent for U(VI) and Th(IV) ions with the previous studies [25–37]. The *Salvadora Persica* branches adsorbent exhibited adsorption capacities 24.85 and 21.21 mg/g for U(VI) and Th(IV) ions respectively, that was by using 0.1 g adsorbent mass which exhibited the highest removal efficiency (shown in Fig. 6) Although the exhibited adsorption capacities by the
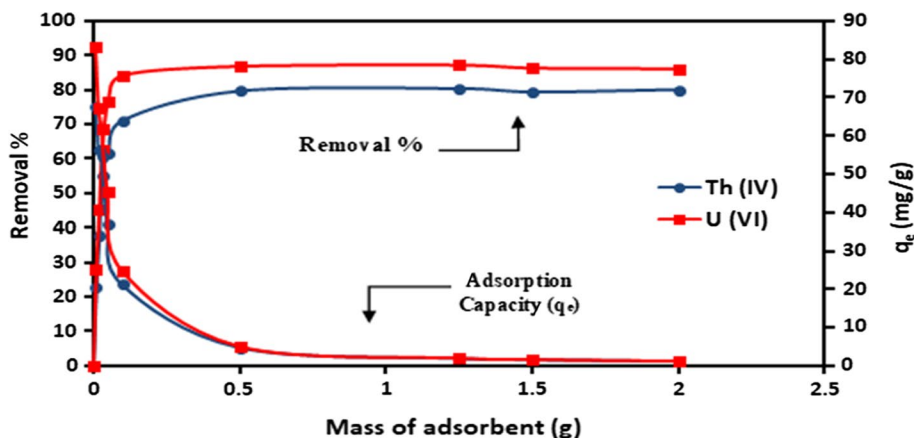
Salvadora Persica branches adsorbent are relatively low, they are comparable with a number of reported values in the literature.

Adsorption of U(VI) and Th(IV)

Figure 7 presents the respective Freundlich and Temkin adsorption isotherms at 25 ± 0.3 °C for U(IV) and Th(IV) on the adsorbent. It is clearly shown in Fig. 7 that the deviation between the experimental and the calculated q_e is lower in the case of fitting by Freundlich isotherm than Temkin isotherm fitting. The results of the linearized isotherms adsorption models (mentioned in Table 1) are represented in Fig. 8.

Table 3 summarizes the calculated isotherms models parameters and the squared correlation coefficients (R^2) for U(VI) and Th(IV) adsorption on the adsorbent. The n value was obtained from the slope of the linear least square fit of ln (q_e) versus ln (C_e), while the K_F value was calculated from the intercept. n and K_F give an idea about the degree of surface heterogeneity and the adsorption capacity of the adsorbent respectively. Larger n and K_F values correspond respectively to greater heterogeneity on the adsorbent's surface and a higher adsorption capacity [38]. The n and K_F values for U(VI) and Th(IV) adsorption indicate that the adsorbent surface heterogeneity and the U(VI) and Th(IV) ions tendency for adsorption are low. For the goodness of fit values (R^2; the squares of the correlation coefficients) of ln (q_e) versus ln (C_e) (linearized Freundlich equation) for U(VI) and Th(IV) ions were better than those obtained R^2 from most of the other linearized forms (i.e. Langmuir, Temkin and R–D isotherms equations). On the other hand, the experimental data for U(VI) and Th(IV) adsorption on *Salvadora Persica* adsorbent fit the Freundlich adsorption isotherm (see Fig. 7a). This indicates that the adsorption of U(VI) and Th(IV) ions is achieved by a physisorption mechanism and the electrostatic interaction between the adsorbent surface and the U(VI) and Th(IV) ions contributed to the adsorption process and these ions form multi-layers

Fig. 6 Comparison between the removal percentage of U(VI) (60 μg/mL) or Th(IV) (60 μg/mL) using the adsorbent at 25 ± 0.3 °C. The secondary axis is the adsorption capacity (q_e)

Table 2 Reported adsorption capacity of different biomass adsorbents for U(VI) and Th(IV)

U(VI)			Th(IV)		
Adsorbent	Q_{max} (mg/g)	Reference	Adsorbent	Q_{max} (mg/g)	References
Coffee residues	40.5	[25]	Rice bran	49.3	[33]
Mangrove endophytic fungus Fusarium sp. #ZZF51	21.42	[26]			
Lemon peel	24.39	[27]	Wheat bran	38.7	
Fresh Spirodela punctata	18.52	[28]	Fusarium sp. #ZZF51	11.4	[34]
Wood fiber	3.93	[29]	Marine-derived Fungus Fusarium sp. #ZZF51	4.72	[35]
Chitin	4.60	[30]	Insolubilized humic acid originated from Azraq	25.32	[36]
Ethylenediamine-modified biomass of Aspergillus niger	4.31 (unmodified) 6.78 (modified)	[31]	Duckweed pyrolytic biochar at 300 °C	86.7	[37]
Elodea nuttallii	3.096	[32]	Duckweed-based pyrolytic biochar at 600 °C	63.5	
Callitriche stagnalis L.	0.112		Salvadora Persica Branches Biomass	21.21	This work
Phragmites australis L.	0.012				
Lemna gibba L.	1.10				
Salvadora Persica branches biomass	24.85	This work			
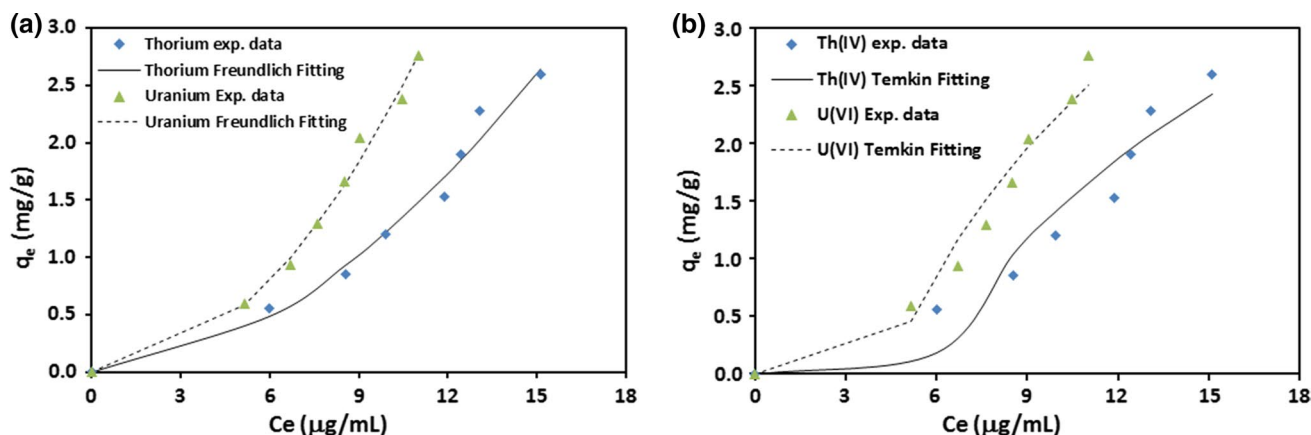
Fig. 7 Adsorption isotherms at 25 ± 0.3 °C for U(IV) and Th(IV) **a** Freundlich isotherm fitting, **b** Temkin isotherm fitting

on the adsorbents. In the Langmuir model, although it shows good linearity, the maximum value of adsorption (Q_0) was negative, which reflects the inadequacy of this model for explaining the adsorption process, [39].

U(VI) and Th(IV) adsorption kinetics

The mechanism of adsorption can be explored by studying the adsorption kinetics. The results presented in Fig. 9 show that, the adsorption rates of U(VI) and Th(IV) reach equilibrium within 2 h. The experimental adsorption capacities ($q_{e,exp}$) for U(VI) and Th(IV) on the adsorbent are given in Table 4. It has been observed most of the U(VI) and Th(IV)

are adsorbed in the first 1 h and slowly reach the equilibrium after 2 h. The initial fast adsorption is attributed to the large number of available active adsorption sites while the slowness at which maximum adsorption is reached is due to the few adsorption sites and the repulsive forces between adsorbate ions in solution and adsorbate ions on the adsorbent. The linear least squares fits of $\ln(q_e - q_t)$ versus t (as shown in Fig. 10a) for the adsorption data of U(VI) and Th(IV) yielded relatively low correlation coefficients (R) those are 0.981 and 0.965 respectively. The calculated adsorption capacity ($q_{e\ Cal}$) of U(VI) and Th(IV) from the pseudo-first order kinetics fits deviated by around 80% and 150% for U(VI) and Th(IV) respectively from the
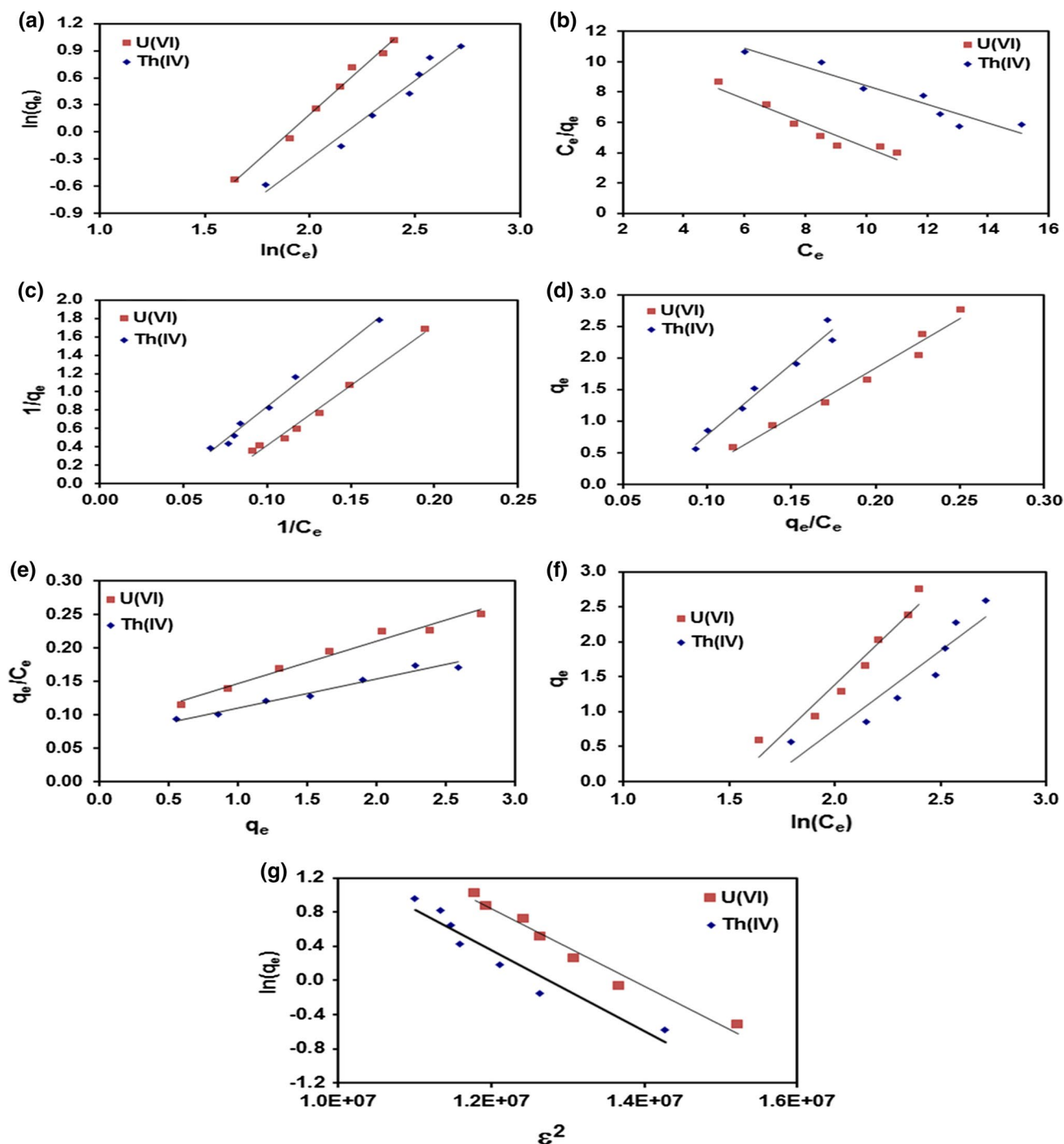
Fig. 8 Linear least squares fit for Linearized **a** Freundlich model, **b** Langmuir linear form type 1, **c** Langmuir linear form type 2, **d** Langmuir linear form type 3, **e** Langmuir linear form type 3, **f** Temkin model, and **g** D-R model for U(IV) and Th(IV) adsorption on adsorbent

experimental adsorption capacity ($q_{e\ \mathrm{exp}}$). On the other hand linear least squares fits of $\frac{t}{q_t}$ versus t (as shown in Fig. 10b) yielded correlation coefficients equal or very close to 1 as well as the $q_{e\ \mathrm{Cal}}$ values are very close to the $q_{e\ \mathrm{exp}}$ (see Table 4) with a deviation % less than 2.5%. This clearly

reveals the adsorption process follows pseudo second order kinetics.

Bearing in mind that the kinetic results fit perfectly into the pseudo second order adsorption kinetics model for U(VI) and Th(IV) on the adsorbent, the diffusion mechanism of these ions was tested and the influence of mass transfer

Table 3 Freundlich, Langmuir, Timken and R-D isotherms models parameters and correlation coefficient for U(VI) and Th(IV) adsorption on *Salvadora Persica* branches adsorbent at 25 ± 0.3 °C

	U(VI)	Th(IV)
Freundlich		
K_f (mg/g)(dm^3/mg)$^{1/n}$	$(1.98 \pm 0.17) \times 10^{-2}$	$(2.29 \pm 0.19) \times 10^{-2}$
n	0.49 ± 0.04	0.57 ± 0.06
R^2	0.990	0.973
Langmuir (1)		
Q_0 (mg/g)	-1.25	-1.64
b	-0.065	-0.042
R^2	0.920	0.918
Langmuir (2)		
Q_0 (mg/g)	-1.13	-1.66
b	-0.068	-0.042
R^2	0.986	0.990
Langmuir (3)		
Q_0 (mg/g)	-1.26	-1.47
b	-0.065	-0.044
R^2	0.975	0.969
Langmuir (4)		
Q_0 (mg/g)	-1.34	-1.57
b	-0.063	-0.043
R^2	0.975	0.969
Temkin		
AT (L/g)	0.995 ± 0.004	0.997 ± 0.003
b_T (J/mol)	841 ± 43	1079 ± 54
R^2	0.947	0.890
D-R		
Q_{max} (mg/g)	539.58	427.32
β (mol^2/kJ^2)	$4.55 \pm 0.02 \times 10^{-7}$	$4.75 \pm 0.03 \, 10^{-7}$
E (kJ/mol)	1.049 ± 0.004	1.026 ± 0.003
R^2	0.970	0.926
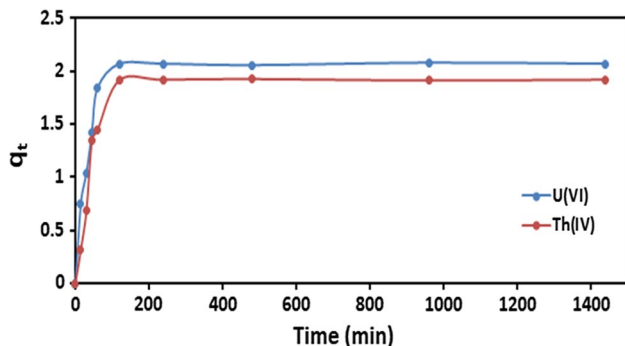
Fig. 9 The effect of contact time on the adsorption capacity (q_t) of U(VI) (60 µg/mL) or Th(IV) (60 µg/mL) using the adsorbent at 25 ± 0.3 °C. The adsorbent amount is 1.25 g

resistance on their binding on the adsorbent was verified using intra-particle diffusion model [40] through using Eq. (7):

$$q_e = k_{id} t^{0.5} + C \tag{7}$$

where k_{id} is the intra-particle diffusion rate constant (mg/g min$^{0.5}$), and C is a constant related to the thickness of the boundary layer (mg/g). Thus, the diffusion constant (k_{id}) can be obtained from the slope of the plot of q_t versus the square root of time.

Figure 11 shows plots of q_t versus $t^{0.5}$ for U(VI) and Th(IV) on adsorbent. These results imply that the adsorption processes involve more than a single kinetic stage or sorption rate [40]. *Salvadora Persica* adsorbent exhibited two stages, the first linear part (first stage) can be attributed to the mass transfer of the adsorbate ions across the boundary layer and intra-particle diffusion, which produces a delay in the adsorption process. The second stage is attributed to the diffusion through small pores, which is followed by the establishment of equilibrium. The presence of micro-pores on the adsorbents is in line with this stage. Table 5 summarizes the calculated values of the diffusion constants for U(VI) and Th(IV) on the adsorbent.

Thermodynamic parameters for U(VI) and Th(IV) adsorption

To further explore the adsorption mechanism, the thermodynamic distribution coefficient (K_d) was calculated at different temperature using Eq. 8, the free energy (ΔG) was calculated using Eq. 9, the enthalpy (ΔH) and entropy of adsorption (ΔS) were calculated using Eqs. 10 from the obtained slope and the intercept respectively of log K_d versus $1/T$ plots (Fig. 12), the results are presented in Table 6.

$$k_d = \frac{q_e}{C_e} \tag{8}$$

$$\Delta G^0 = RT \ln k_d \tag{9}$$

$$\ln K_d = \frac{\Delta S^0}{R} - \frac{\Delta H^0}{RT} \tag{10}$$

The positive value of ΔG at all temperatures for the adsorption of U(VI) as well as Th(IV) confirms that the adsorption process of those ions on the adsorbent is non-spontaneous and thermodynamically unfavorable. However, the negative ΔH values and the decrease of ΔG with increasing the temperature indicate that the adsorption of U(VI) and Th(IV) is an exothermic process. The adsorption mechanism can be classified as chemisorption, physisorption or mixed mechanism based on the value of ΔH and ΔG. The adsorption process is described as physisorption when the ΔH is less negative than -40 kJ mol^{-1} and the absolute value of

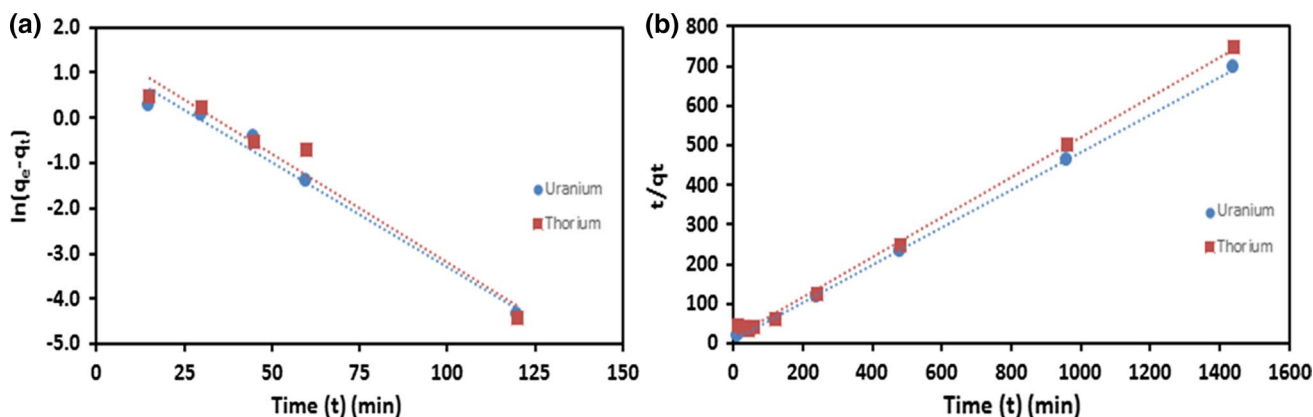| Table 4 Pseudo-first order and Pseudo-Second order kinetics parameters for U(VI) or Th(IV) adsorption on the *Salvadora Persica* adsorbent		Pseudo-first order			Pseudo-second order		
	$q_{e\ \text{exp.}}$	R^2	$q_{e\ \text{Cal}}$	k_1	R^2	$q_{e\ \text{Cal}}$	k_2
U(VI)	2.08	0.9818	3.74	1.06×10^{-1}	0.9996	2.10	3.14×10^{-2}
Th(IV)	1.93	0.9651	4.88	1.10×10^{-1}	0.9970	1.98	1.68×10^{-2}

Fig. 10 a) Pseudo-first order and b) Pseudo-second order sorption kinetics of U(IV) and Th(IV) onto the adsorbent at 25 ± 0.3 °C and pH = 4
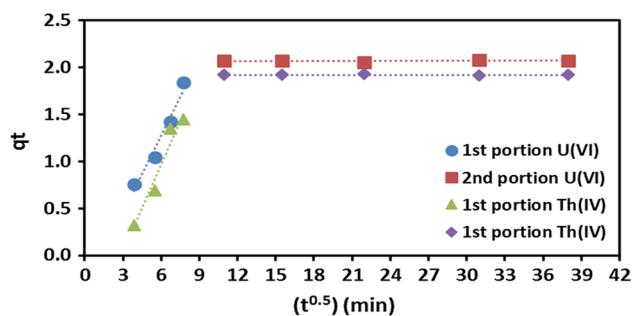

Fig. 11 Plots of q_t versus $t^{0.5}$ showing the two diffusion stages predicted by the diffusion model for U(VI) (square and circle ligand) and Th(IV) (pyramidal and rhombic ligand) adsorption on the adsorbent

Fig. 12 Plots of $\ln K_d$ versus $1/T$ for U(VI) and Th(IV) on the adsorbent at pH = 4.0

Table 5 Intra-particle diffusion parameters for U(VI) and Th(IV) ions on the adsorbent

Ions	Intra-particle Diffusion Parameters		
	K_{id}	C	R^2
U(VI)	0.0286	1.2626	0.4591
Th(IV)	0.0342	0.9533	0.4671

ΔG is lower than 20 kJ mol^{-1}. On the other hand, the process is classified as a chemisorption when the absolute value of ΔG is higher than 40 kJ mol^{-1} and the ΔH is lower than -100 kJ mol^{-1}. However, if ΔG is lower than 40 kJ mol^{-1} and higher than 20 kJ mol^{-1}, the adsorption mechanism classified a mixed mechanism [41, 42]. The calculated values of
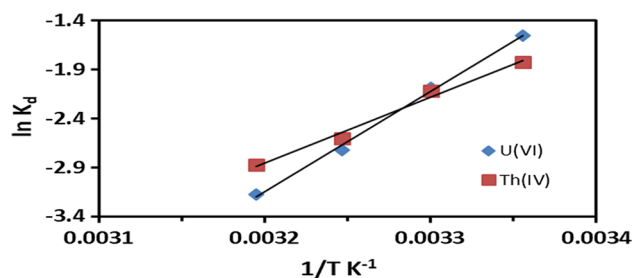
ΔG are ranging in between 3.86 and 8.26 kJ mol^{-1}, and the ΔH values for the adsorption of the U(VI) and Th(IV) ions were found to be -85.16 ± 3.50 and -55.95 ± 4.41 kJ mol^{-1} respectively. This suggests that the adsorption is attained through a mixed mechanism and dominated by a physisorption mechanism. The small negative values of ΔS for the adsorption of uranium and thorium confirm the little decrease of randomness at the solid/liquid interface during the adsorption, where the adsorbed ions displaced the adsorbed water molecules on the surface of adsorbent [4].

Conclusion

In this study, for the first time, the *Salvadora Persica* Branches low-cost biosorbent was investigated for the removal of U(VI) as well as Th(IV) from aqueous media

Table 6 Thermodynamic parameters for adsorption of U(VI) and Th(IV) by adsorbent material

Temperature (°C)	U(VI)			Th(IV)		
	ΔG (kJ mol⁻¹)	ΔH (kJ mol⁻¹)	ΔS (kJ mol⁻¹)	ΔG (kJ mol⁻¹)	ΔH (kJ mol⁻¹)	ΔS (kJ K⁻¹)
25	3.86	-85.16 ± 3.50	-0.30 ± 0.01	4.53	-55.95 ± 4.41	-0.20 ± 0.01
30	5.26			5.34		
35	6.98			6.66		
40	8.26			7.47		

at pH 3. The results showed that the Freundlich isotherm model is the best to describe the equilibrium data and the kinetics of the adsorption follows the pseudo-second order and the adsorption process involves two kinetics stages (i.e. mass transfer across the boundary layer followed by the diffusion through the micro-pores and establishing the equilibrium). The adsorption mechanism of U(VI) and Th(IV) radioactive ions on the adsorbent was found to be attained through a mixed mechanism and dominated by a physisorption mechanism. However, the adsorption of these ions was non-spontaneous and thermodynamically unfavorable with a small positive value of ΔG. The adsorption process of these ions was exothermic with an enthalpy driven process with negative values of ΔH (-85.16 kJ mol⁻¹) for U(VI) and -55.95 kJ mol⁻¹ for Th(IV).

Compliance with ethical standards

References

1. Majdan M, Pikus S, Gajowiak A, Gładysz-Płaska A, Krzyżanowska H, Żuk J, Bujacka M (2010) Characterization of uranium(VI) sorption by organobentonite. Appl Surf Sci 256(17):5416–5421

2. Kumar Amit, Ali Manjoor, Pandey Badri N (2013) Understanding the biological effects of thorium and developing efficient strategies for its decorporation and mitigation. BARC Newsletter 335:55–60

3. Kim JS, Han KS, Kim SJ, Kim S-D, Lee J-Y, Han C, Kumar JR (2016) Synergistic extraction of uranium from Korean black shale ore leach liquors using amine with phosphorous based extractant systems. J Radioanal Nucl Chem 307(2):843–854

4. Bayyari MA, Nazal MK, Khalili FI, Asoudani E (2017) Synergistic effect of tri-n-butyl phosphate (TBP) or tri-n-octyl phosphine oxide (TOPO) with didodecylphosphoric acid (HDDPA) on extraction of uranium(VI) and thorium(IV) ions. J Radioanal Nucl Chem 312(1):133–139

5. Bayyari MA, Nazal MK, Khalili FI (2010) The effect of ionic strength on the extraction of thorium(IV) from perchlorate solution by didodecylphosphoric acid (HDDPA). Arab J Chem 3(2):115–119

6. Bayyari MA, Nazal MK, Khalili FI (2010) The effect of ionic strength on the extraction of Thorium(IV) from nitrate solution by didodecylphosphoric acid (HDDPA). J Saudi Chem Soc 14(3):311–315

7. Anirudhan TS, Rijith S, Tharun AR (2010) Adsorptive removal of thorium(IV) from aqueous solutions using poly(methacrylic acid)-grafted chitosan/bentonite composite matrix: process design and equilibrium studies. Colloids Surf A 368(1–3):13–22

8. Ioannou K, Hadjiyiannis P, Liatsou I et al (2019) U(VI) adsorption by biochar fiber-MnO₂ composites. J Radioannal Nucl Chem 320:425–432. https://doi.org/10.1007/s10967-019-06479-9

9. Jie Yu, Luo Xuegang, Liu Bo, Zhou Jian, Feng Jian, Zhu Wenkun, Wang Shanlin, Zhang Yongde, Lina Xiaoyan, Chen Ping (2018) Bayberry tannin immobilized bovine serum albumin nanospheres: characterization, irradiation stability and selective removal of uranyl ions from radioactive wastewater. J Mater Chem A 6:15359–15370

10. Baybaş D, Ulusoy U (2011) The use of polyacrylamide-aluminosilicate composites for thorium adsorption. Appl Clay Sci 51(1–2):138–146

11. Khalili F, Al-Banna G (2015) Adsorption of uranium(VI) and thorium(IV) by insolubilized humic acid from Ajloun soil–Jordan. J Environ Radioact 146:16–26

12. Mahanani Erlina Sih, Samuel Samantha Victoria (2007) MISWAK (*Salvadora persica*) as a cleansing teeth. Mutiara Medika 7(1):38–42

13. Ileri O, Cay S, Erduran N (2014) Removal of common heavy metals from aqueous solutions by waste *Salvadora persica* L. branches (Miswak). Int J Environ 8(4):987–996

14. Savvin SB (1961) Analytical use of arsenazo III: determination of thorium, zirconium, uranium and rare earth elements. Talanta 8(9):673–685

15. Freundlich HMF (1906) Over the adsorption in solution. J Phys Chem 57:385–471

16. Langmuir I (1916) The constitution and fundamental properties of solids and liquids. J Am Chem Soc 38(11):2221–2295

17. Temkin MI, Pyzhev V (1940) Kinetics of ammonia synthesis on promoted iron catalyst. Acta Phys Chim USSR 12:327–356

18. Dada AO, Olalekan AP, Olatunya AM, Dada O (2012) Langmuir, freundlich, temkin and Dubinin–Radushkevich isotherms studies of equilibrium sorption of Zn2 + unto phosphoric acid modified rice husk. IOSR J Appl Chem 3(1):38–45

19. Lagergren S (1898) Zur theorie der sogenannten adsorption gelöster stoffe Kungliga Svenska Vetenskapsakademiens. Handlingar 24(4):1–39

20. Ho YS, McKay G (1998) A comparison of chermosorption kinetic models applied to pollutant removal on various sorbents. Trans IChemE 76:332–340

21. Bawazeer Tahani M, Alsoufi Mohammad S, Katowah Dina, Alharbi Waad S (2016) Effect of aqueous extracts of *Salvadora*

persica "Miswak" on the acid eroded enamel surface at nano-mechanical scale. Mater Sci Appl 7:754–771

22. Halib Nadia, Nuairy Nabilah Bt, Ramli Haslinda, Ahmad Ishak, Othman Norinsan Kamil, Salleh Salihatun Md, Bakarudin Saiful Bahari (2017) Preliminary Assessment of *Salvadora persica* whitening effects on extracted Stained teeth. J Appl Pharm Sci 7(12):121–125

23. Wang J, Hu X, Liu Y, Xie SB, Bao ZL (2010) Biosorption of uranium(VI) by immobilized *Aspergillus fumigatus* beads. J Environ Radioactiv 101(6):504

24. Xia LS, Tan KX, Wang X, Zheng WN (2010) Adsorption behavior of uranium and mechanism analysis on banyan leaves. At Energy Sci Technol 44(3):278

25. Mahramanlioglu M, Bicer IO, Misirli T, Kilislioglu A (2007) Removal of uranium by the adsorbents produced from coffee residues. J Radioanal Nucl Chem 273:621–624

26. Yang HB, Tan N, Wu FJ, Liu HJ, Sun M, She ZG, Lin YC (2012) Biosorption of uranium(VI) by a mangrove endophytic fungus Fusarium sp. #ZZF51 from the South China Sea. J Radioanal Nucl Chem 292:1011–1016

27. Šabanović Elma, Muhić-Šarac Tidža, Nuhanović Mirza, Memić Mustafa (2019) Biosorption of uranium(VI) from aqueous solution by citrus limon peels: kinetics, equilibrium and batch studies. J Radioanal Nucl Chem 319:425–435. https://doi.org/10.1007/s10967-018-6358-3

28. Nie X, Dong F, Liu M, Sun S, Yang G, Zhang W, Qin Y, Ma J, Huang R, Gong J (2016) Removel of uranium from aqueous solutions by spirodela punctata as the mechanism of biomineralization. Procedia Environ Sci 31:382

29. Wang Z, Yi FC, Feng Y (2015) Adsorption behavior and mechanism of uranium on wood fiber. At Energy Sci Technol 49:263–272

30. Sunilkumar B, Chakrapani G (2014) Studies on sorption of uranium on chitin: a solid-state extractant application for removal of uranium from ground water. J Radioanal Nucl Chem 302:1489–1493

31. Ding D, Xin X, Li L, Hu N, Li G, Wang Y, Fu P (2014) Removal and recovery of U(VI) from low concentration radioactive wastewater by ethylenediamine-modified biomass of *Aspergillus niger*. Water Air Soil Pollut 225:2206–2222

32. Yang H, Luo X, Ding H, Zhang X (2019) Adsorption of U(VI) by *Elodea nuttallii*: equilibrium, kinetic and mechanism analysis. J Radioanal Nucl Chem 319:227–235

33. BoveiriMonji A, Ghoulipour V, Mallah MH, Maraghe-Mianji B (2015) Selective sorption of thorium(IV) from highly acidic aqueous solutions by rice and wheat bran. J Radioanal Nucl Chem 303:949–958

34. Yang SK, Tan N, Yan XM, Chen F, Lin YC (2013) Adsorption of thorium(IV) from aqueous solution by non-living biomass of mangrove endophytic fungus Fusarium sp. #ZZF51. J Radioanal Nucl Chem 298:827–833

35. Yang SK, Tan N, Wu WLX, Hou J, Xiang KX, Lin YC (2015) Biosorption of thorium(IV) from aqueous solution by living biomass of marine-derived fungus Fusarium sp. #ZZF51. J Radioanal Nucl Chem 306:99. https://doi.org/10.1007/s10967-015-4060-2

36. Khalili FI, Khalifa A, Al-Banna G (2017) Removal of uranium(VI) and thorium(IV) by insolubilized humic acid originated from Azraq soil in Jordan. J Radioanal Nucl Chem 311:1375

37. Ting C, Nan Z, Zhao X, Xin H, Zhuhong D (2019) Integrated comparisons of thorium(IV) adsorption onto alkali-treated duckweed biomass and duckweed-derived hydrothermal and pyrolytic biochar. Environ Sci Pollut Res 26:2523–2530

38. Li L, Quinlivan PA, Knappe DRU (2002) Effects of activated carbon surface chemistry and pore structure on the adsorption of organic contaminants from aqueous solution. Carbon 40:2085–2100

39. Alshabanat M, Alsenani G, Almufarij R (2013) Removal of crystal violet dye from aqueous solutions onto date palm fiber by adsorption technique. J Chem. https://doi.org/10.1155/2013/210239

40. Weber WJ, Morris JC (1963) Kinetics of adsorption on carbon from solution. Journal of the Sanitary Engineering Division. 89(2):31–60

41. Larabi L, Harek Y, Traisnel M, Mansri A (2004) Inhibition behavior of mild steel in 1 M HCl in the presence of poly(4-vinylpyridine) (P4VP) and potassium iodide. J Appl Electrochem 34:833–839

42. El-Awady GY, El-Said IA, Fouda AS (2008) Anion surfactants as corrosion inhibitors for aluminum dissolution in HCl solutions. Int J Electrochem Sci 3:174–190